

CHAPTER 4

EXCESS PROTON SOLVATION AND DELOCALIZATION IN A HYDROPHILIC POCKET OF THE PROTON CONDUCTING POLYMER NAFION

Reprinted with permission from the American Chemical Society

(Petersen, M.K., Wang, F., Blake, N.P., Metiu, H., Voth, G.A., 2005. J. Phys. Chem. B
109, 3727-3730)

Excess Proton Solvation and Delocalization in a Hydrophilic Pocket of the Proton Conducting Polymer Membrane Nafion

Matt K. Petersen,[†] Feng Wang,[†] Nick P. Blake,[‡] Horia Metiu,[‡] and Gregory A. Voth^{*,†}

Department of Chemistry and Center for Biophysical Modeling and Simulation, University of Utah, 315 S. 1400 E. Rm. 2020, Salt Lake City, Utah 84112-0850, and Department of Chemistry and Biochemistry, University of California, Santa Barbara, California 93106-9510

Received: December 1, 2004; In Final Form: January 28, 2005

Solvation properties of the hydrated excess proton are studied in a hydrophilic pocket of Nafion 117 through a series of molecular dynamics simulations. The multistate empirical valence bond (MS-EVB) methodology, which enables the delocalization of the excess proton through the Grotthuss hopping mechanism, was employed for one of the excess protons in the simulation cell. Simulations were performed such that “classical” nondissociable hydronium cations and a single excess proton treated with the MS-EVB methodology were at a concentration ratio of 39:1. Two degrees of hydration of the Nafion polymer electrolyte membrane were simulated, each displaying the same marked difference between the solvation structures of the classical versus MS-EVB treated (Grotthuss shuttling) excess proton species. These differences are attributed to the solvent dynamics needed to transfer the cation between the solvent separated and contact pair positions about the sulfonic acid counterion. The results demonstrate that it is generally impossible to describe the low pH conditions in the hydrophilic domains of Nafion without the explicit treatment of Grotthuss delocalization in the underlying molecular dynamics model for the excess protons.

There has been a great deal of interest in proton conducting membranes as an integral component of polymer electrolyte membrane (PEM) fuel cells. In particular Nafion, the preferred polymeric membrane for hydrogen and methanol fuel cells, has been the subject of numerous theoretical^{1–4} and experimental^{5–9} studies. Nafion is composed of sulfonic acid terminated perfluorovinyl ether pendants regularly spaced along a perfluorinated backbone. Both simulation^{2–4} and experiment^{7–9} suggest that hydrated Nafion consists of hydrophobic and hydrophilic domains. The hydrophobic regions are composed of the perfluoroalkyl backbone of the polymer, while the hydrophilic ones contain water, the sulfonic acid groups of the side chains (see Figure 1), and excess protons. The mobility of the excess protons through the hydrophilic domains is presumed to be very high.

The high proton mobility of Nafion is thought to be facilitated by the Grotthuss^{10,11} shuttling mechanism in which the excess proton is transferred from one water molecule to another by a series of chemical and hydrogen bonding rearrangements. The standard classical empirical force fields used in most molecular dynamics (MD) computer simulations cannot adequately describe this bonding rearrangement. In contrast, this behavior can be described by the multistate empirical valence bond (MS-EVB) model. A two-state empirical valence bond model for proton hopping in water was first developed by Lobaugh and Voth¹² and later improved by extension to multiple states by Schmitt and Voth.^{13,14} A second-generation model (MS-EVB2) was further developed by Day et al.¹⁵ and has been shown to give a good description of the proton transport potential energy

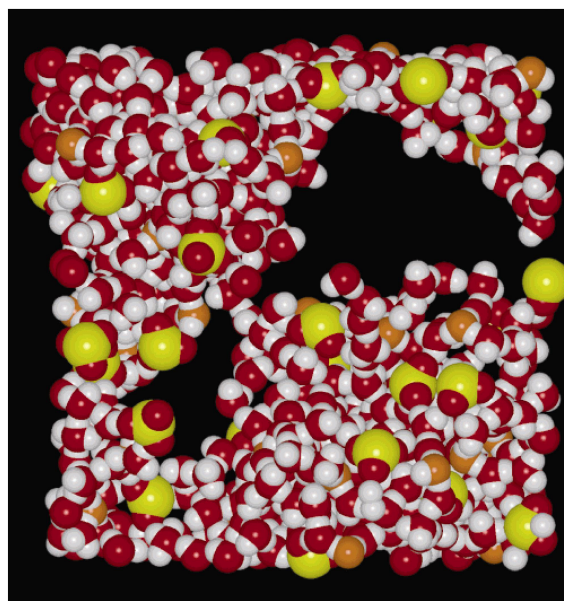


Figure 1. Representative configuration of the distribution of water, hydronium ions, and sulfonate ions within the simulation unit cell.^{22,23} The voids are occupied by the Nafion backbone and the perfluorovinyl ether pendant. Red spheres are water and sulfonate oxygens. White spheres are water and hydronium hydrogens. Yellow spheres are sulfonate sulfurs. Orange spheres are hydronium oxygens.

surface, in reasonable agreement with ab initio results and experimental measurements. In this communication we report

* Corresponding author. E-mail: voth@chem.utah.edu

[†] University of Utah.

[‡] University of California, Santa Barbara.

results from a series of molecular dynamics (MD) simulations of Nafion 117 employing the MS-EVB2 model. Previous simulations¹⁶ of excess protons in Nafion have used a potential that is an approximation to the MS-EVB2 model, so it does not describe fully the Grotthuss proton shuttling behavior. One of the main goals of this communication is to explore to what extent the properties of the excess proton and the water in the hydrophilic channels are modified when the Grotthuss process and the associated proton delocalization is described more accurately.

Aside from its technological importance Nafion is also scientifically interesting. The material in the hydrophilic domains is geometrically confined and the ion concentration is extremely high. Both factors disrupt the hydrogen-bonding network of water and hinder the ability of water to fully solvate all ions. This is bound to lead to unusual water structure and ion solvation. The high ionic concentration and the confinement also affect proton mobility. The presence of a large number of SO_3^- ions, tied to the domain walls, will diminish it and the quasi-one-dimensionality of the system may enhance it. To determine the net outcome of these conflicting tendencies we need to use reliable, nonclassical interactions. The focus in this work is primarily on the solvation structure of the excess proton and, in particular, how the Grotthuss delocalization process affects that solvation. Limited dynamical (diffusion) results will also be presented, but this is a more subtle and difficult issue which will be the focus of future research.

Our simulations use four Nafion 117 chains, each of which contains 10 equally spaced monomers. The polymer portion of the potential was described by the force field recently employed by Jang et al.,³ while the water portion, as well as explicit proton transport, was described by the MS-EVB2 model.^{13–15} The MS-EVB2 and polymer potentials were mixed using the Lorentz–Berthelot mixing rules, and the Ewald summation method was employed for all electrostatic interactions. It has been demonstrated^{1,7} that even at very low hydration levels the excess proton is fully dissociated from the sulfonic acid group. For this reason, we included no protonated sulfonic groups in our simulations (i.e., these chemically bonded protonated configurations were not included in the MS-EVB2 model).

Two systems of differing hydration were created having a water-to-acid ratio (λ) of 7 and 15. Each was constructed by starting with randomly placed water, polymer, and classical hydronium cations with approximately 50% of the experimental density, using periodic boundary conditions. A constant temperature equilibration was carried out for 500 ps at 400 K followed by 1 ns of a constant pressure/temperature equilibration at 300 atm and 1 K. The densities after annealing were found to be in agreement with that obtained in a previous simulation³ and within 6% ($\rho_{\lambda=15} = 1.61 \text{ g/cm}^3$) and 9% ($\rho_{\lambda=7} = 1.70 \text{ g/cm}^3$) of the experimental values.¹⁷ From each annealed configuration, 10 distinct trajectories were started by randomly replacing one classical hydronium molecule with a hydronium cation to be treated with the MS-EVB2 model; all other protons were treated with classical empirical potentials. Each starting configurations was used to generate a 200 ps trajectory with the temperature maintained at 300 K using the Nose–Hoover thermostat with a relaxation time of 0.5 ps. From these trajectories a total of 2 ns of data at each hydration level was collected for analysis. Strictly speaking, MD calculations of self-diffusion rates should be carried out by running Newton’s equations in the microcanonical (constant NVE) ensemble. However, we have found that such rates are the same to within statistical error when instead we use the Nose–Hoover equations of motion, so long as the

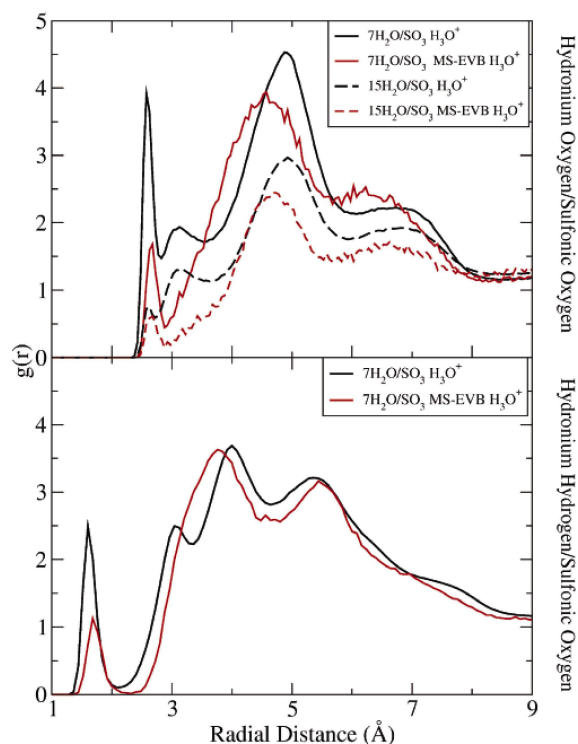


Figure 2. (top panel) Radial distribution functions between the oxygen in the hydronium cation and the oxygen atoms in the SO_3^- group at hydrations of $\lambda = 7$ and $\lambda = 15$. The red lines are obtained by using the pivot oxygen in MS-EVB method, and the black lines were obtained by using the classical potential. (bottom panel) Radial distributions between the hydrogen atoms in the hydronium cation and the oxygen atoms in the SO_3^- group at a hydration of $\lambda = 7$.

energy conservation of microcanonical trajectories for the MS-EVB2 model is stable.

In our simulations certain structural properties, for example the marked hydrophilic/hydrophobic phase separation of Nafion, are similar to those found in other studies.^{2,3} However, most noteworthy in the present study is the *dissimilar solvation structure* between the two possible types of ion pairs. In particular, the oxygen radial distributions between the sulfonic acid oxygens with both the proton shuttling MS-EVB2 and nonproton shuttling classical hydronium oxygen are shown in Figure 2, top panel. The relative concentration of the contact ion pair (CIP), which is responsible for the first sharp peak around 2.75 Å, to the solvent separated ion pair (SSIP), which is responsible for the largest peak around 4.75 Å, is significantly different between the classical hydronium and MS-EVB2 descriptions. Integration of these radial distributions indicate the concentration of the CIP in the classical hydronium description is approximately twice that observed for the MS-EVB2 model for the least hydrated simulation; however, this ratio approaches 1:1 for the more hydrated simulation. The larger CIP concentration of the classical hydronium model at low hydration is attributed to the greater affinity for water of the MS-EVB hydronium in the first solvation shell; hence sulfonic acid groups are displaced by water in this region. As the hydration is increased the concentrations for the CIP of the two different cations converge.

The distinct peak at ~ 3.2 Å in the classical hydronium radial distribution also distinguishes the two cations. This feature is conspicuously absent in the MS-EVB curves. Analysis of the

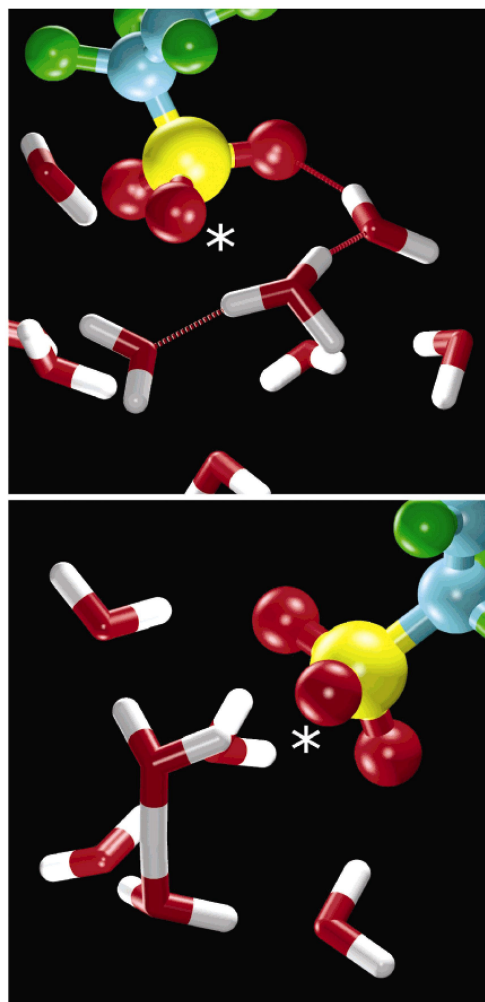


Figure 3. (top panel) Representative configuration of the “intermediate” solvation structures observed in the simulations using the classical hydronium potential.^{22,23} Note the water molecule hydrogen bonded (H-bonds in red) to the oxygen adjacent to the inspected oxygen (asterisk). Extraneous hydrogen bonds, water molecules, and polymer were excluded for clarity. (bottom panel) Representative configuration of the Zundel structure observed in the simulations using the MS-EVB2 potential. Relative to the inspected oxygen (asterisk) one water of the Zundel cation is located in the contact ion pair (CIP) position, while the other is located in the solvent separated ion pair (SSIP) position.

trajectories indicates a weak correlation between the dipole of the sulfonic group and the dipole of the hydronium ion in this region, with a marginal preference for antiparallel configurations. A distance of 3.2 Å is certainly too long to allow direct hydrogen bonding to the hydronium ion and the sulfonic acid oxygen. Further inspection reveals that these configurations are typified by “bridging” water molecules (Figure 3, top panel) that are hydrogen bonded to both the classical hydronium and a neighboring oxygen of the *same* sulfonic acid group, with the sulfonic oxygen participating in no hydrogen bonds. When a solvating water occupies the hydrogen bonding position on this sulfonic oxygen the hydronium is unable to occupy this intermediate position and instead is found in the solvent separated position. We suggest that these configurations may represent local minima between the CIP and the SSIP. The solvent reorganization required by the classical model to allow

for the transition between the CIP and the SSIP is clearly a deficiency, since that model does not allow for rearrangement of the covalent and hydrogen bond configurations. A goal of this study is to contrast the classical and MS-EVB potentials in order to show the need for a model that allows bonding rearrangements (Grotthuss shuttling), so we have chosen not to investigate these artificial peaks further.

The MS-EVB proton CIP to SSIP transition requires little solvent reorganization because the excess proton can shuttle through the hydrogen bond network. A Zundel-like (H_5O_2^+) cation configuration predominates when the MS-EVB2 proton is adjacent to a sulfonic acid group. One water of the Zundel cation is hydrogen bonded to a sulfonic oxygen, while the other is located away from SO_3^- (bottom panel, Figure 3). The proton easily moves away from the sulfonic ion through a Grotthuss shuttle between these two water molecules. Experimental evidence exists for this kind of depletion of the Eigen-type solvation structure in favor of the Zundel-type for other concentrated strong acids, i.e., concentrated HCl solutions.^{18,20} Simulations recently performed with the new self-consistent iterative multi-state empirical valence bond (SCI-MS-EVB) method,²⁰ which is capable of simulating multiple excess protons, has replicated this enhancement of the Zundel solvation structure over the Eigen-type. In the context of these experimental results, a classical hydronium potential seems clearly deficient.

The bottom panel of Figure 2 shows the distribution functions the classical and MS-EVB2 hydronium hydrogen atoms from the sulfonic acid oxygen for the low hydration simulation. The distinguishing feature of the MS-EVB2 curve is the broad feature, which replaces the peak around 3 Å in the classical simulation. This peak in the classical simulation is composed of the hydronium hydrogens of the CIP hydronium that are not directly hydrogen bonded to the sulfonic acid oxygen, as well as the hydrogens of the hydronium in the intermediate position (top panel, Figure 3) as described above. Since the Zundel cation predominates in the CIP region for the MS-EVB2 simulation, the distinction between the hydrogens coming from the CIP hydronium and those from the SSIP hydronium is blurred (bottom panel, Figure 3). There is also no appreciable contribution to the MS-EVB2 radial distribution from these intermediate hydronium configurations.

Figure 4 illustrates the diffusion coefficients for all proton containing species as a function of hydration. It has been previously shown¹⁵ that the self-diffusion of the water potential used in the MS-EVB2 model is approximately 30% larger than the experimental value and, not unexpectedly, the water diffusion for this Nafion simulation is also larger than experiment⁶ for both degrees of hydration. Conversely, the diffusion of the MS-EVB2 excess proton in bulk water was shown in earlier work to be roughly half of the bulk experimental value, and, in turn, the classical hydronium was shown to be about half of the MS-EVB2 excess proton diffusion value.¹⁵ This trend also extends to these simulations and the corresponding experimental⁶ data. In the present simulations, one likely reason for the apparent under estimation of the diffusion constant of the Grotthuss shuttling proton by the MS-EVB2 model (certainly in the least hydrated simulation) is the effect of “caging” by the classical hydroniums. The MS-EVB2 proton is artificially trapped in a cage formed by classical hydroniums that, in turn, cannot participate in the Grotthuss hopping process important for the proton transport. When the level of Nafion hydration is increased, thereby increasing the distance between the cations and the extent of the bonding network, the ratio between the

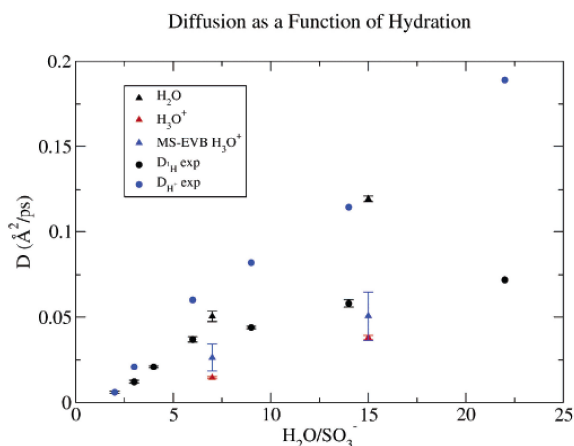


Figure 4. Diffusion coefficients for simulation (triangle) and experiment (circle). The blue and black circles represent experimental¹⁶ values for the charged protons and all protons, respectively. The black, red, and blue triangles represent simulation values for water, classical hydronium, and the Grotthuss shuttling excess proton described by the MS-EVB2 model, respectively.

experimental diffusion and that of the Grotthuss shuttling MS-EVB2 proton decreases from 2.8 to the previously demonstrated¹⁵ bulk value of 2.3 for the MS-EVB2 model. It should be noted that the diffusion data reported here are not to be taken too literally because the system is in essence “artificial” in the sense that most of the excess protons are treated as classical hydronium cations (i.e., they cannot participate in Grotthuss shuttling). The main purpose of this work is to reveal some of the significant features coming from the delocalization of an excess proton in the Nafion hydrophilic pocket, primarily in its solvation structure. To adequately study the excess proton diffusion, *all* excess protons will need to be treated as Grotthuss protons, e.g., through the use of the SCI-MS-EVB model.²⁰ Furthermore, a description of the macroscopic proton diffusion requires a connection to be made between the atomistic-scale proton diffusion and the percolation of the water network between the hydrophilic Nafion pockets.³ Both aspects of the problem will be the focus of future work.

We note the difference between the simulated underlying water diffusion and the experimental value is more pronounced for the more hydrated simulation. Due to the delocalized nature of the excess proton in the MS-EVB2 method, the solvating waters exhibit a stronger binding over those of the classical hydronium. The large difference in experimental and simulated water diffusion is partially attributed to this underestimated binding of the water molecules by the classical hydroniums. Interestingly, this is consistent with femtosecond pump–probe near-IR experiments,²¹ which indicate that the first solvation shell of aqueous ions has characteristically slower reorientation times than those in bulk water. By contrast, the water in the first solvation shell of the classical hydronium is more mobile than in the case of the delocalized MS-EVB2 hydronium, and this leads, in part, to the disparity between the simulated and experimental water diffusion values. It is expected that a simulation using a full SCI-MS-EVB treatment for all excess

protons will bring the water diffusion more in line with the experimental value. A molecular dynamics code implementing the SCI-MS-EVB method for the tractable treatment of multiple dissociable protons has recently been developed²⁰ and will be the focus of our future efforts.

In summary, simulations of Nafion 117 at two different hydration levels were reported in this communication using both classical hydronium ions and an MS-EVB2 treatment of a single excess proton. Distinct differences were found in the radial distribution functions of the classical and MS-EVB2 cations, such as an apparently artificial peak in the classical hydronium/sulfonic oxygen radial distribution. This latter peak is attributed to the inability of the classical model to transfer protons between the two moieties of the Zundel cation via Grotthuss shuttling. Furthermore, we suggest that at low hydration the proton diffusion calculated for an MS-EVB2 proton is artificially reduced by the caging from the classical hydroniums in the simulation cell. These artifacts, arising from the limitations of the classical hydronium description, highlight the need for a model that allows Grotthuss shuttling (i.e., dynamical changes in the hydrogen and chemical bond topology) for *all* excess protons. Further work in this direction is in progress.

Acknowledgment. This material is based upon work supported by the U. S. Army Research Laboratory and the U. S. Army Research Office under grant number DAAD 19-03-1-0121.

References and Notes

- (1) Paddison, S. J. *J. New Mater. Electrochem. Systems* **2001**, *4*, 197.
- (2) Vishnyakov, A.; Neimark, A. V. *J. Phys. Chem. B* **2001**, *105*, 9586.
- (3) Jang, S. S.; Molinero, V.; Cagin, T.; Goddard, W. A., III. *J. Phys. Chem. B* **2004**, *108*, 3149.
- (4) Elliott, J. A.; Hanna, S.; Elliot, A. M. S.; Cooley, G. E. *Phys. Chem. Chem. Phys.* **1999**, *1*, 4855.
- (5) Paddison, S. J.; Paul, R.; Zawodzinski T. A. *J. Chem. Phys.* **2001**, *115*, 1753.
- (6) Zawodzinski, T. A.; Neeman, M.; Sillerud, L. O.; Gottesfeld, S. *J. Phys. Chem.* **1991**, *95*, 6040.
- (7) Laporta, M.; Pegoraro, M.; Zanderighi, L. *Phys. Chem. Chem. Phys.* **1999**, *1*, 4619.
- (8) Rollet, A. L.; Diat, O.; Gebel, G. *J. Phys. Chem. B* **2002**, *106*, 3033.
- (9) Loppinet, B.; Gebel, G.; Williams, C. E.; *J. Phys. Chem. B* **1997**, *101*, 1884.
- (10) Agmon, N. *Chem. Phys. Lett.* **1995**, *244*, 456.
- (11) Bell, R. P. *The Proton in Chemistry*; Cornell University Press: Ithaca, New York, 1973.
- (12) Lobaugh, J.; Voth, G. A. *J. Chem. Phys.* **1996**, *104*, 2056.
- (13) Schmitt, U. W.; Voth, G. A. *J. Chem. Phys.* **1999**, *111*, 9361.
- (14) Cuma, M.; Schmitt, U. W.; Voth, G. A.; *J. Phys. Chem. A* **2001**, *105*, 2814.
- (15) Day, T. J. F.; Soudackov, A. V.; Cuma, M.; Schmitt, U. W.; Voth, G. A. *J. Chem. Phys.* **2002**, *117*, 5839.
- (16) Spohr, E.; Commer, P.; Kornyshev, A. A. *J. Phys. Chem. B* **2002**, *106*, 10560.
- (17) Morris, D. R.; Xiaodong, S. *J. Appl. Polym. Sci.* **1993**, *50*, 1445.
- (18) Agmon, N. *J. Phys. Chem. A* **1998**, *102*, 192.
- (19) Kameda, Y.; Usuki, T.; Uemura, O. *Bull. Chem. Soc. Jpn.* **1998**, *71*, 1305.
- (20) Wang, F.; Voth, G. A., in press.
- (21) Omta, A. W.; Kropman, M. F.; Woutersen, S.; Bakker, H. J. *Science* **2003**, *301*, 347.
- (22) Illustrations created with the visualization package VMD.; Humphrey, W.; Dalke, A.; Schulten, K. *J. Mol. Graphics* **1996**, *14*, 33.
- (23) Illustrations rendered with Raster3D.; Merritt, E. A.; Murphy, M. E. P. *Acta Crystallogr.* **1994**, *D50*, 869.